

Scientific Report No. 73

COUPLED MODE THEORY OF TWO NON-PARALLEL
DIELECTRIC WAVEGUIDES*

by

Mark A. McHenry and David C. Chang

January 1983

Electromagnetics Laboratory
Department of Electrical Engineering
University of Colorado
Boulder, Colorado 80309

*This work is supported by the U.S. Army Research Office under grant no. DAAG29-82-K-0096, monitored by Dr. James Mink.

COUPLED MODE THEORY OF TWO NON-PARALLEL
DIELECTRIC WAVEGUIDES[†]

Mark A. McHenry
and
David C. Chang^{††}

Abstract

A general theory for treating the coupling between two non-parallel dielectric waveguides is developed using the coupled mode assumption. This theory is used to analyze directional couplers consisting of two circularly curved, single mode dielectric slab waveguides. By assuming continuous coupling between the two waveguides rather than only between adjacent segments on the two waveguides, the present theory avoids the awkwardness of having to specify in a somewhat arbitrary manner the separation between these segments as is the case for existing theories reported in the literature. It is shown that this oversimplification results often in an over estimate of the power transfer in a directional coupler by 10-20% compared to this theory.

[†]This work is supported by U.S. Army Research Office under grant no. DAAG29-82-K-0096, monitored by Dr. James Mink.

^{††}The authors are with the Electromagnetics Laboratory, Department of Electrical Engineering, University of Colorado, Boulder, CO 80309. (The first author is now with Northrop Corp., Hawthorne, CA 90250.)

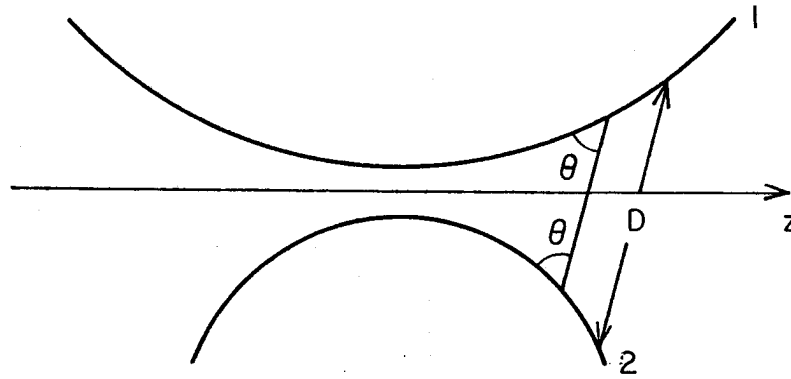
1. Introduction

The coupling between dielectric waveguides has received much attention [1-6] in the last decade in light of the development of fiber optics and more recently, integrated circuits in the optical and millimeter wave bands. Devices needed for future systems such as directional couplers require that the coupling between waveguides be understood so performance can be optimized and cut and try development minimized. Although coupling between parallel guides has been well understood for some time [7,8], coupling between nonparallel guides is still not clearly understood even though any physically realizable device must have nonparallel connecting sections where coupling takes place.

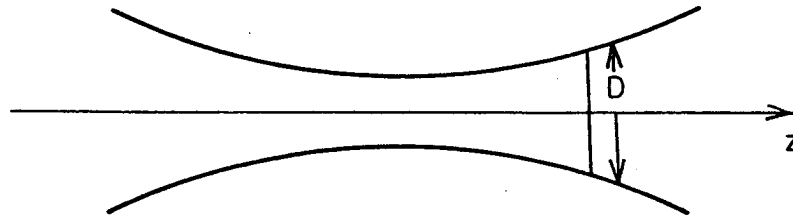
Making the coupled mode assumption, many authors use the results of the parallel case (i.e., the amount of coupling is dependent on guide separation and other parameters describing each guide in isolation), and postulate that in a nonparallel configuration, there exists a one-to-one correspondence between segments on each guide with some function giving a "separation" to use in the parallel results.

Matsuhara and Watanabe [4] assume this distance is given along a line that intersects the guides at equal angles (Fig. 1 a). Abouzahra and Lewin [3] for the symmetric case give the distance separating the guides along a line normal to the plane of symmetry (Fig. 1 b) while Trinh and Mittra [2] use the length of an arc intersecting both guides at right angles (Fig. 1 c).

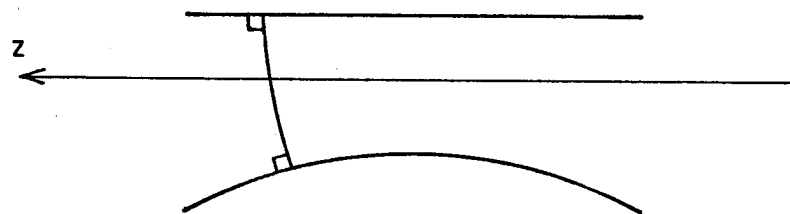
By trying to stretch the results of the parallel case we find not only this problem of determining the "correct" separation, but we overlook the real physical process of interacting time dependent fields. In the parallel case, any z cross section will have fields with constant



(a)



(b)



(c)

Fig. 1. Various definitions for separation between individual segments of two parallel guides

phase, while in the nonparallel situation, the phase will not be constant and will change as the configuration on either side of the cross section is changed. Considering only some type of separation between the guides will not completely describe the coupling because the effect one guide has on another will depend very strongly on the phase as well as the strength of the overlapping fields.

In this paper, coupled mode theory is developed to describe any configuration where the coupled mode approximation is valid. Approximate coupling coefficients for circularly bend, lossless, single TE mode slab waveguides are worked out allowing analysis of directional couplers composed of straight and circularly bent slab waveguides.

2. Coupled Mode Theory of Two Nonparallel Waveguides

The configuration to be analyzed is shown in Fig. 2. The two guides can have different cross section A_1 and A_2 and dielectric constants ϵ_1 and ϵ_2 but the permeability (μ) is uniform; $\bar{E}_1, \bar{A}_1, \bar{E}_2, \bar{H}_2$ are the two surface-wave mode fields each guide supports if the other guide is not there; \tilde{E} and \tilde{H} are the time fields we are interested in, that of both guides together. We then define the functions $\epsilon_1(x,y,z)$, and $\epsilon_2(x,y,z)$ to represent the variation in the relative permittivities when only guide 1 and guide 2, respectively, is presented, i.e.

$$\epsilon_{1,2}(x,y,z) = \begin{cases} \epsilon_{1,2} & \text{when } \bar{x} \in A_{1,2} \\ \epsilon_3 & \text{otherwise} \end{cases}$$

Note that $\epsilon_1(x,y,z) = \epsilon_3$ (not ϵ_2) in the region guide 2 occupies and vice versa. $\tilde{\epsilon}(x,y,z)$ is the relative permittivity when both guides are together.

The vectors \bar{F}_1 and \bar{F}_2 can then be defined^[1]

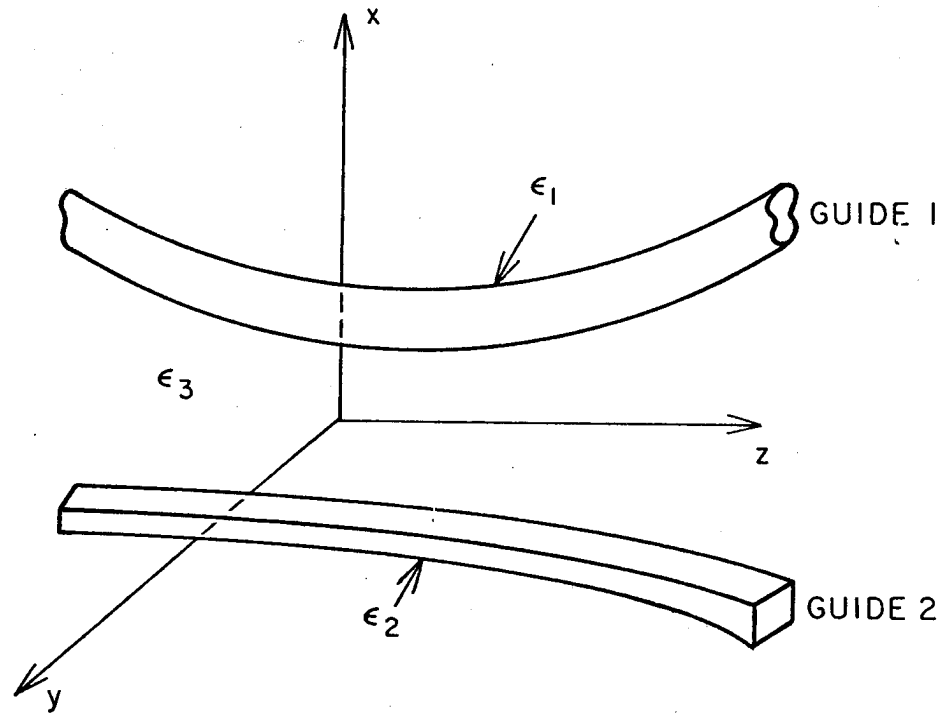


Fig. 2. Two non-parallel dielectric waveguides.

$$\bar{F}_{1,2} = \bar{E}_{1,2} \times \tilde{H}^* + \tilde{E}^* \times \bar{H}_{1,2} \quad (1)$$

By using Maxwell's equations and vector identities it can be shown that

$$\nabla \circ \bar{F}_{1,2} = j\omega\epsilon_0 (\tilde{\epsilon} - \epsilon_{1,2}) \bar{E}_{1,2} \circ \tilde{E}^* \quad (2)$$

Making the usual couple-mode assumption that the total field of a system of two waveguides can be approximated in any given cross section by a linear combination of the individual mode fields

$$\tilde{E} = m_1(z) \bar{E}_1 + m_2(z) \bar{E}_2 \quad (3)$$

$$\tilde{H} = m_1(z) \bar{H}_1 + m_2(z) \bar{H}_2 \quad (4)$$

where m_1 and m_2 are the amplitudes of the two modes at z . Using the vector identity [1] over an infinite cross section A ,

$$\int_A \nabla \circ \bar{F} dA = \frac{\partial}{\partial z} \int_A \bar{F} \circ \hat{z} dA \quad (5)$$

we get a set of coupled differential equations for $m_1(z)$ and $m_2(z)$.

$$\begin{aligned} & j[m_1^*(z) A_{1,2}(z) + m_2^*(z) B_{1,2}(z)] \\ & = \frac{\partial}{\partial z} [m_1^*(z) C_{1,2}(z) + m_2^*(z) D_{1,2}(z)] \end{aligned} \quad (6)$$

where A, B, C, D are cross-sectional integrals relating the two individual mode fields:

$$A_{1,2}(z) = \int_{-\infty}^{\infty} \int_{-\infty}^{\infty} (\tilde{\epsilon}(x,y,z) - \epsilon_{1,2}(x,y,z)) \bar{E}_{1,2} \circ \bar{E}_1^* dx dy \quad (7)$$

$$B_{1,2}(z) = \int_{-\infty}^{\infty} \int_{-\infty}^{\infty} (\tilde{\epsilon}(x,y,z) - \epsilon_{1,2}(x,y,z)) \bar{E}_{1,2} \circ \bar{E}_2^* dx dy \quad (8)$$

$$C_{1,2}(z) = \frac{1}{\omega \epsilon_0} \iint_{-\infty}^{\infty} [\bar{E}_{1,2} \times \bar{H}_1^* + \bar{E}_1^* \times \bar{H}_{1,2}] \cdot \hat{z} \, dx \, dy \quad (9)$$

$$D_{1,2}(z) = \frac{1}{\omega \epsilon_0} \iint_{-\infty}^{\infty} [\bar{E}_{1,2} \times \bar{H}_2^* + \bar{E}_2^* \times \bar{H}_{1,2}] \cdot \hat{z} \, dx \, dy \quad (10)$$

In general, the coupling coefficients are complex functions of z except for C_1 and D_2 which are real normalization parameters. (C_1 and C_2 are constants for guides that don't radiate energy to infinity.)

If the z dependence of each guide in isolation is $\exp[-j\beta_{1,2} z_{1,2}]$, the coupling coefficients of parallel configurations will have simple $\exp[-j\beta' z]$ z dependence ($\beta' = \text{constant, possibly zero}$). In the nonparallel case the integration on x at constant z includes a new term of the form $\exp[-j\beta' [z_1 - z_2]]$ where $z_1 - z_2$ now is a function of x . This phase term accounts for the interference of the modal fields which, in the parallel case, doesn't exist because all phase fronts are parallel.

Theories currently in the literature either assume the coupling coefficients are the same as the parallel case except now the separation is changing in some arbitrary manner [3,4], or the amount of power transferred depends on the spacing as in the parallel case and define some "equivalent" separation to use at each z cross section [2]. Both approaches neglect field interference in the coupling coefficients which, as shown later, can lead to significant errors.

We note that the use of equivalent current sources [9] or in the parallel case, the use of variational methods to find the propagation constant of the system modes [8] would appear to give different results. However, we have shown in [10] that coupled mode assumption actually leads to identical expressions for these approaches.

3. Analysis of Couplers Formed with Circularly Curved Slab Waveguides

Figure 3 shows the two lossless, single TE mode, circularly bend slab waveguides and the relationship between the different coordinate systems. We assume that the radius of curvature of the slabs is large enough so that the field of the bent guide in isolation is approximately that of a straight guide curved about a point. The fields of each guide in isolation are given in Appendix A. To evaluate the coupling coefficients $A_{1,2}$, $B_{1,2}$, $C_{1,2}$ and $D_{1,2}$ in (6), we have to relate the coordinate system for the guides, (x_1, z_1) and (x_2, z_2) , to the globe coordinate system as follows:

$$x_{1,2} = \pm R_{1,2} \left[1 - \sqrt{\left(1 + \frac{D}{2R_{1,2}} \mp \frac{x}{R_{1,2}}\right)^2 + \left(\frac{z}{R_{1,2}}\right)^2} \right] \quad (11)$$

$$z_{1,2} = R_{1,2} \tan^{-1} \left[\frac{z/R_{1,2}}{1 + \frac{D}{2R_{1,2}} \mp \frac{x}{R_{1,2}}} \right] \quad (12)$$

$$\sin \theta_{1,2} = \frac{z}{\sqrt{\left(R_{1,2} + \frac{D}{2} \mp x\right)^2 + z^2}} \quad (13)$$

$$\cos \theta_{1,2} = \frac{R_{1,2} + \frac{D}{2} \mp x}{\sqrt{\left(R_{1,2} + \frac{D}{2} \mp x\right)^2 + z^2}} \quad (14)$$

Simplifying the expression for the coupling coefficients, we note that the major contribution to the coupling coefficient integrals comes mainly from areas near the guides. Also, to avoid radiation losses, the radius of curvature of the bent slab waveguide inherently must be large. These two facts allow us to expand equations linearly in x about each of the guides [10] and find analytic solutions for the integrals in (7) - (10) (Appendix C). For example,

$$x_1 = \begin{cases} S_{11}(z) + T_{11}(z) \cdot x & x > 0 \text{ (near guide 1)} \\ S_{12}(z) + T_{12}(z) \cdot x & x < 0 \text{ (near guide 2)} \end{cases} \quad (15)$$

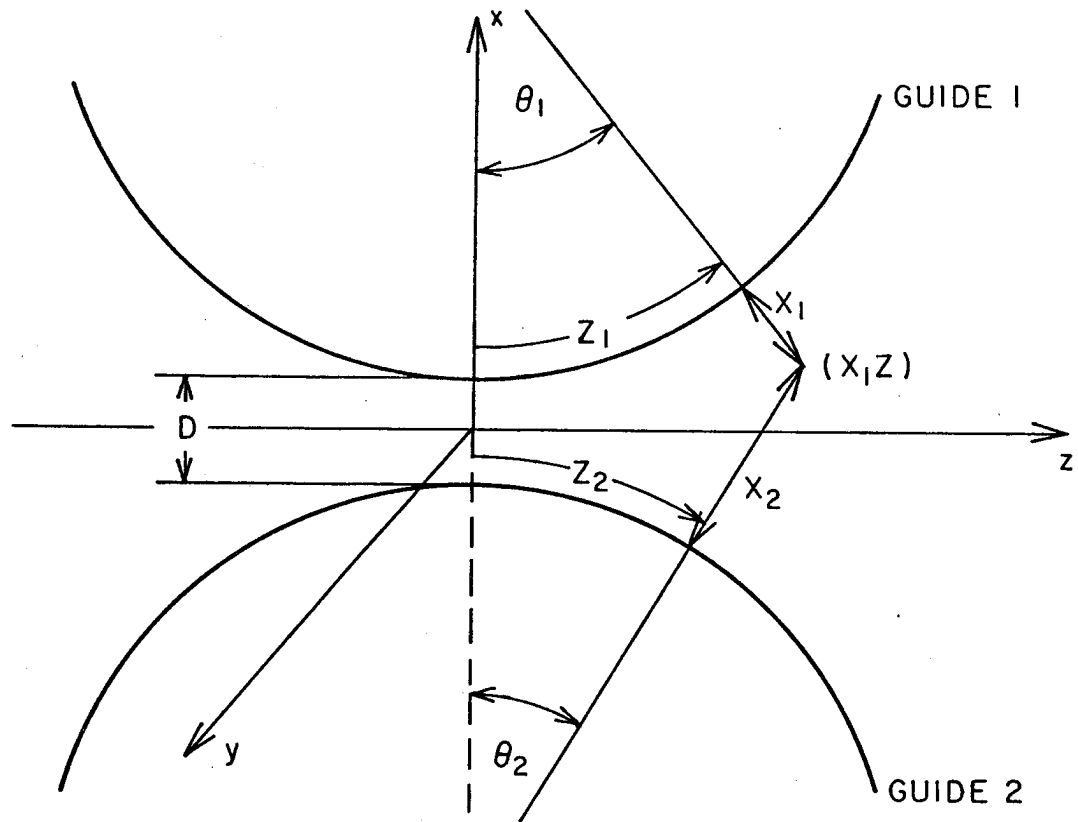


Fig. 3. Global and local coordinate systems

where S_{1j} and T_{1j} are given in Appendix B. To solve the remaining coupled differential equations, a second order Runge Kutta [11] algorithm was used. The approximate coupling coefficients were compared with "exact" numerical integration of these integrals and found to be within 5% of the true values for the cases shown here. Seven seconds on a Cyber 6400 was required for analysis of a configuration carrying all the coupling coefficients.

4. Numerical Results

Figures 4 and 5 show that the final power in guide 1 vs. γd (unit power in Guide 1 and none in Guide 2 initially) for the present theory, Abouzahra-Lewin [3] and Trinh-Mittra [2].[†] Both symmetric and nonsymmetric cases show the reduced amount of coupling the present theory predicts compared with other theories.

It is seen that the further assumption of one-to-one correspondence of the coupling depending on the separation of the two nonparallel guides, as was true in the parallel case, can lead to significant errors when the minimum normalized separation between the two guides, λd , is smaller. To further demonstrate this point, we have included in Fig. 6 the coupling coefficient B_1 for a symmetrically, curved, degenerate coupler normalized by the constant C_1 . In the parallel degenerate case, B_1/C_1 would be a real constant with exponential dependence on guide separation. In all the conventional theories for nonparallel guides which don't account for the phase term, B_1/C_1 would

[†] Comparison with Yariv [12] on a coupler with long parallel section and negligible coupling in the curved sections shows Trinh and Mittra's (k) is missing a factor of $1/(1+1/\gamma a)$. With this correction, we let the factor (v) be equal to 1 for all cases here.

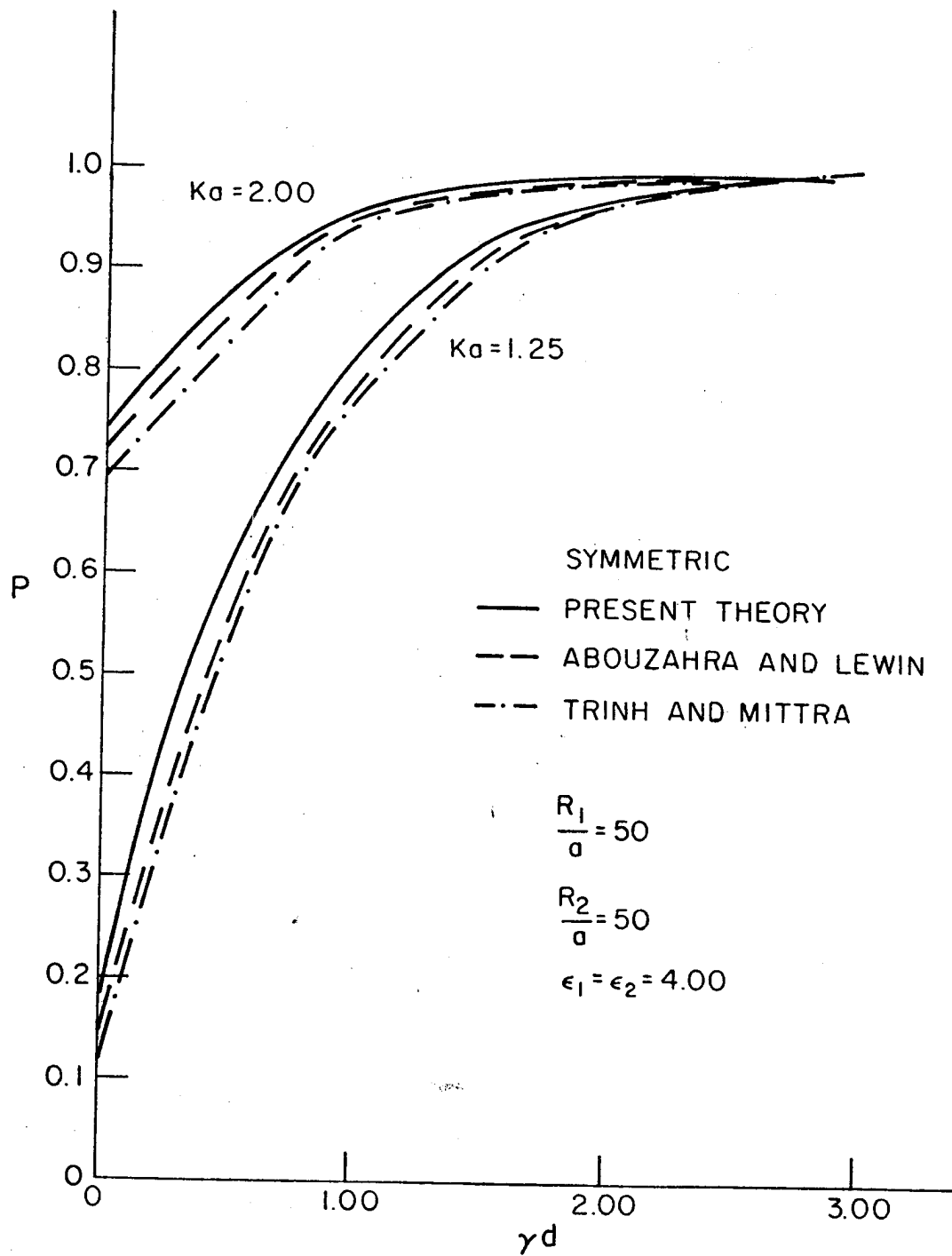


Fig. 4. Final power at Guide 1 vs. separation

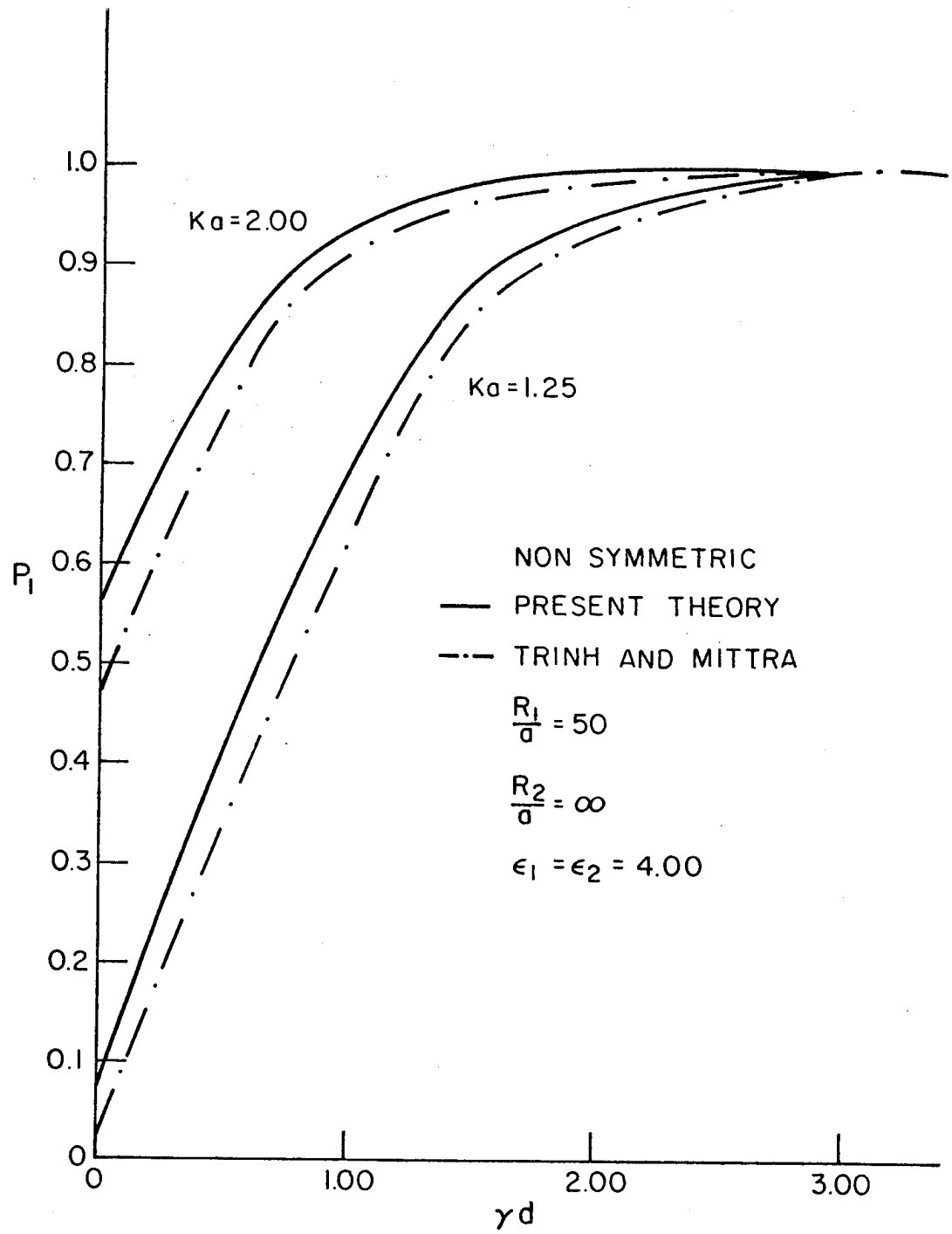


Fig. 5. Final power at Guide 1 vs. separation

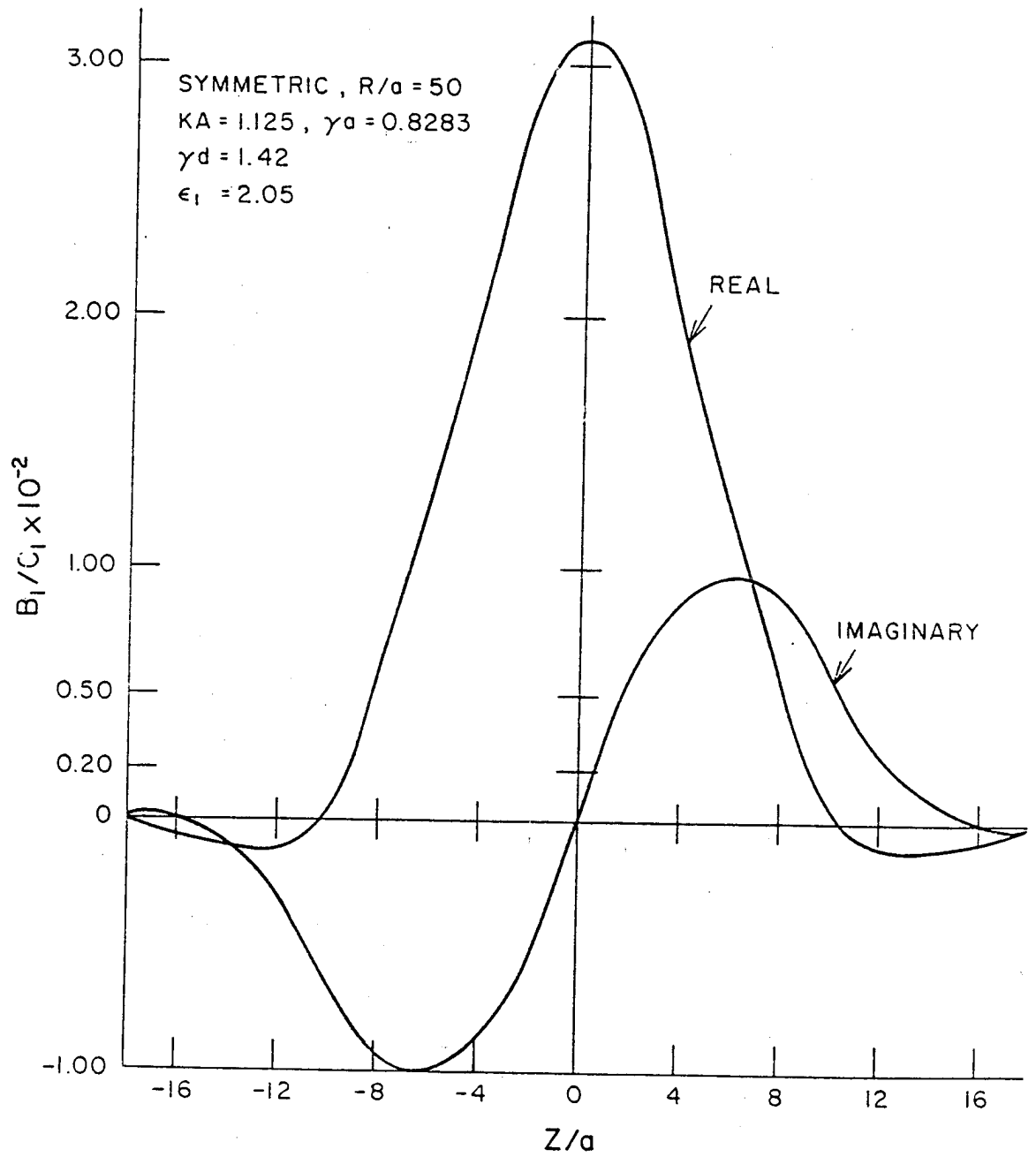


Fig. 6. Coupling coefficient ratio B_1/C_1 vs. Z/a

be a real function that exponentially decayed on either side of $z=0$ (minimum guide separation). This type of difference exists in the other coupling coefficients and leads to the discrepancies of the theories.

It is of interest to note that we found the total power was not conserved along the coupler for two very closely-spaced guides where λd is much smaller than 1, or the physical separation is less than the penetration depth. This likely indicates a breakdown in the coupled mode approximation that includes only one surface-wave mode on each guide. This means, as it stands, none of the existing theories really is adequate in designing a circular coupler that provides a complete transfer of power.

APPENDIX A

Field of Each Guide in Isolation

Each guide in isolation is a lossless slab structure supporting a single TE mode. The two guides have the same cross-section, the same uniform permittivity and are excited at the same frequency. With these assumptions, the field of either guide in isolation will be [8]

$$\left. \begin{aligned} E_{y_i} &= \cos p x_i e^{-j\beta z_i} \\ H_{z_i} &= -\frac{p}{\omega\mu_0} \sin p x_i e^{-j\beta z_i} \\ H_{x_i} &= -\frac{\beta}{\omega\mu_0} \cos p x_i e^{-j\beta z_i} \end{aligned} \right\} |x_i| < a \quad (A.1)$$

$$\left. \begin{aligned} E_{y_i} &= \cos pa e^{\gamma a} \exp(-\gamma|x_i|) e^{-j\beta z_i} \\ H_{z_i} &= \frac{x_i j\gamma}{|x_i| \omega\mu_0} \cos pa e^{\gamma a} \exp[-\gamma|x_i|] e^{-j\beta z_i} \\ H_{x_i} &= \frac{\beta}{\omega\mu_0} \cos pa e^{\gamma a} \exp[-\gamma|x_i|] e^{-j\beta z_i} \end{aligned} \right\} |x_i| > a \quad (A.2)$$

$$p^2 = k_0^2 \epsilon_i - \beta^2$$

$$\gamma^2 = \beta^2 - k_0^2 \epsilon_3 \quad (A.3)$$

$$\tan pa = \frac{\gamma}{p} .$$

APPENDIX B

LINEAR APPROXIMATION OF x_1

$$x_1 \approx \begin{cases} S_{11}(z) + T_{11}(z) & x > 0 \text{ (near guide 1)} \\ S_{12}(z) + T_{12}(z) & x < 0 \text{ (near guide 2)} \end{cases} \quad (\text{B.1})$$

$$S_{1j} = R_1 - \sqrt{\left(R_1 + \frac{D}{2} - \Delta_j\right)^2 + z^2} - \frac{\Delta_j \left(R_1 + \frac{D}{2} - \Delta_j\right)}{\left(R_1 + \frac{D}{2} - \Delta_j\right)^2 + z^2} \quad (\text{B.2})$$

$$T_{1j} = \frac{R_1 + \frac{D}{2} - \Delta_j}{\sqrt{\left(R_1 + \frac{D}{2} - \Delta_j\right)^2 + z^2}} \quad (\text{B.3})$$

where

$$\Delta_1 = R_1 + \frac{D}{2} - \sqrt{R_1^2 - z^2} \quad (\text{B.4})$$

$$\Delta_2 = - \left(R_2 + \frac{D}{2} - \sqrt{R_2^2 - z^2}\right) \quad (\text{B.5})$$

APPENDIX C

APPROXIMATE COUPLING COEFFICIENTS

By use of the linear approximations similar to those of Appendix B and the isolated field equations, Appendix A, the coupling coefficients (7)-(10) for lossless, degenerate but not necessarily symmetric configurations can now be directly integrated with the following comments.

Equations (7)-(10) calls for the vector fields in the x, y, z coordinate system. For the TE case, the following is easily shown:

$$\bar{E}_i = (0, E_{y_i}, 0) \quad (C.1)$$

$$\bar{H}_1 = (H_{x_1} \cos \theta_1 + H_{z_1} \sin \theta_1, 0, -H_{x_1} \sin \theta_1 + H_{z_1} \cos \theta_1) \quad (C.2)$$

$$\bar{H}_2 = (H_{x_2} \cos \theta_2 - H_{z_2} \sin \theta_2, 0, H_{x_2} \sin \theta_2 + H_{z_2} \cos \theta_2) \quad (C.3)$$

where H_{x_1} , H_{x_2} , H_{z_1} and H_{z_2} are part of the isolated field equations in Appendix A.

The integrals for A_1 , A_2 , B_1 and B_2 are only over guide 1 or guide 2 since

$$\tilde{\epsilon}(x, y, z) - \epsilon_{1,2}(x, y, z) = \begin{cases} 0 & \text{elsewhere} \\ (\epsilon_3 - \epsilon_{2,1}) & \text{in guide 2,1} \end{cases} \quad (C.4)$$

All the coefficients have been divided by the half width of the guide (a).

All lengths are in terms of the guide half width.

$$A_1 = \frac{(\epsilon_2 - \epsilon_3) \cos^2(pa) e^{2\gamma a} \left[1 + S_{12} - \frac{T_{12}}{T_{22}} S_{22} \right] \sinh \left[2\gamma a \frac{T_{12}}{T_{22}} \right]}{\gamma a \cdot T_{12}} \quad (C.5)$$

$$\begin{aligned}
B_1 = & (\epsilon_2 - \epsilon_3) \cos(pa) e^{\gamma a} e^{\gamma a [S_{12} - \frac{T_{12}}{T_{22}} S_{22}]} e^{-j\beta a [v_2 - u_2 \frac{S_{22}}{T_{22}}]} \\
& \cdot \frac{2}{(pa T_{22})^2 + (\beta' a)^2} \left[\beta' a \sinh \left[\frac{\beta' a}{T_{22}} \right] \cos pa \right. \\
& \left. + pa \cdot T_{22} \cosh \left[\frac{\beta' a}{T_{22}} \right] \sin pa \right] \quad (C.6)
\end{aligned}$$

where

$$\beta' a = \gamma a T_{12} - j\beta a u_2$$

$$C_1 = \frac{2\beta a}{(ka)^2} \left[1 + \frac{1}{\gamma a} \right] \quad (C.7)$$

$$D_1 = D_1' + D_1'' + D_1''' + D_1'''' \quad (C.8)$$

$$D_1' = \sum_{i=1}^4 \int \frac{B(i)}{A(i)} \exp[G3(i)x][Q(i) + O(i)x] dx \quad (C.9)$$

$$M(1) = N(1) = N(2) = N(3) = 1 \quad (C.10)$$

$$M(2) = M(3) = M(4) = N(4) = -1 \quad (C.11)$$

$$P(i) = \frac{\cos pa}{ka^2} \exp[\beta a(2 - N(i)S_2 - M(i)S_1 - j\beta aV)] \quad (C.12)$$

$$Q(i) = P(i)[\beta a(J_1 + J_2) - \gamma a j[M(i)F_1 + N(i)F_2]] \quad (C.13)$$

$$O(i) = P(i)[\beta a(K_1 + K_2) - \gamma a j[M(i)G_1 + N(i)G_2]] \quad (C.14)$$

$$G3(i) = -\gamma a[M(i)T_1 + N(i)T_2] - j\gamma aU \quad (C.15)$$

$$B(1) = \infty \quad A(1) = (1 - S_1)/T_1$$

$$B(2) = (1 - S_1)/T_1 \quad A(2) = 0 \quad (C.16)$$

$$B(3) = 0 \quad A(3) = (1 - S_2)/T_2$$

$$B(4) = (-1 - S_2)/T_2 \quad A(4) = -\infty$$

where in (C.12) through (C.16), if $i = 1$ or 2 , the linear approximations (S, T, J, K, \dots) around guide 1 should be used while if $i = 3$ or 4 , the approximations about guide 2 should be used.

$$D_1'' = \sum_{i=1}^2 Q(i) \int_{-1}^1 \exp[G_3(i)x] \sin[pa x] dx \quad (C.17)$$

$$G_3(1) = \gamma a [T_{12}/T_{22} - j\beta a U_2/T_{22}] \quad (C.18)$$

$$G_3(2) = -\gamma a [T_{21}/T_{11} - j\beta a U_1/T_{22}] \quad (C.19)$$

$$Q(1) = -\cos(pa) \exp(\gamma a) pa / ka^2 (F_{22} + G_{22} \Delta_2) / T_{22} \\ \cdot \exp[\gamma a (S_{12} - T_{12} \cdot S_{22}/T_{22}) - j\beta a (V_2 - U_2 S_{22}/T_{22})] \quad (C.20)$$

$$Q(2) = \cos(pa) \exp(\gamma a) pa / ka^2 (F_{11} + G_{11} \Delta_1) / T_{11} \\ \cdot \exp[-a (S_{21} - T_{21} S_{11}/T_{11}) - j\beta a (V_1 - U_1 S_{11}/T_{11})] \quad (C.21)$$

$$D_1''' = \frac{\beta a}{ka^2} \left[(J_{11} + J_{21} + \Delta_1 (K_{11} + K_{21})) \frac{A_2^*}{\epsilon_1 - \epsilon_3} \right. \\ \left. + (J_{12} + J_{22} + \Delta_2 (K_{12} + K_{22})) \frac{B_1}{\epsilon_2 - \epsilon_3} \right] \quad (C.22)$$

$$D_1''' = \frac{j\gamma a}{ka^2} \left[(F_{12} + \Delta_2 G_{12}) \frac{B_1}{\epsilon_2 - \epsilon_3} - (F_{21} + \Delta_1 G_{21}) \frac{A_2^*}{\epsilon_1 - \epsilon_3} \right] \quad (C.23)$$

$$A_2 = (\epsilon_1 - \epsilon_3) \cos(pa) e^{\gamma a} e^{\gamma a [-S_{21} + \frac{T_{21}}{T_{11}} S_{11}]} e^{-j\beta a [-V_1 + \frac{S_{11}}{T_{11}} U_1]}$$

$$\cdot \frac{2}{(pa T_{11})^2 + (\beta' a)^2} \left[\beta' a \sinh \left[\frac{\beta' a}{T_{11}} \right] \cos pa \right. \\ \left. + pa T_{11} \cosh \left[\frac{\beta' a}{T_{11}} \right] \sin pa \right] \quad (C.24)$$

where

$$\beta'a = -\gamma_a T_{21} + j\beta_a U_1$$

$$B_2 = -(\epsilon_1 - \epsilon_3) \frac{\cos^2 pa}{\gamma_a T_{21}} \exp\left[2\gamma_a\left(1 - S_{21} + \frac{T_{21}}{T_{11}} S_{11}\right)\right] \sinh\left[-2\gamma_a \frac{T_{21}}{T_{11}}\right] \quad (C.25)$$

$$C_2 = D_1^* \quad (\text{by inspection of equations (9) and (10)}) \quad (C.26)$$

$$D_2 = C_1 \quad (\text{by symmetry}) \quad (C.27)$$